Stoichiometric Production of Hydrogen Peroxide and Parallel Formation of Ferric Multimers through Decay of the Diferric−Peroxo Complex, the First Detectable Intermediate in Ferritin Mineralization†

Guy N. L. Jameson,‡ Weili Jin,§ Carsten Krebs,‡,|| Alice S. Perreira,‡,⊥ Pedro Tavares,‡,⊥ Xiaofeng Liu,§ Elizabeth C. Theil,*,§ and Boi Hanh Huynh*,‡

Department of Physics, Emory University, Atlanta, Georgia 30322, and Children's Hospital Oakland Research Institute, 5700 Martin Luther King Jr. Way, Oakland, California 94609-1673

Received July 18, 2002; Revised Manuscript Received September 8, 2002

ABSTRACT: The catalytic step that initiates formation of the ferric oxy−hydroxide mineral core in the central cavity of H-type ferritin involves rapid oxidation of ferrous ion by molecular oxygen (ferroxidase reaction) at a binuclear site (ferroxidase site) found in each of the 24 subunits. Previous investigators have shown that the first detectable reaction intermediate of the ferroxidase reaction is a diferric−peroxo intermediate, F_{peroxo}, formed within 25 ms, which then leads to the release of H_2O_2 and formation of ferric mineral precursors. The stoichiometric relationship between F_{peroxo}, H_2O_2, and ferric mineral precursors, crucial to defining the reaction pathway and mechanism, has now been determined. To this end, a horseradish peroxidase-catalyzed spectrophotometric method was used as an assay for H_2O_2. By rapidly mixing apo M ferritin from frog, Fe^{2+}, and O_2 and allowing the reaction to proceed for 70 ms when F_{peroxo} has reached its maximum accumulation, followed by spraying the reaction mixture into the H_2O_2 assay solution, we were able to quantitatively determine the amount of H_2O_2 produced during the decay of F_{peroxo}. The correlation between the amount of H_2O_2 released with the amount of F_{peroxo} accumulated at 70 ms determined by Mössbauer spectroscopy showed that F_{peroxo} decays into H_2O_2 with a stoichiometry of 1 F_{peroxo}:H_2O_2. When the decay of F_{peroxo} was monitored by rapid freeze−quench Mössbauer spectroscopy, multiple diferric μ-oxo/μ-hydroxo complexes and small polynuclear ferric clusters were found to form at rate constants identical to the decay rate of F_{peroxo}. This observed parallel formation of multiple products (H_2O_2, diferric complexes, and small polynuclear clusters) from the decay of a single precursor (F_{peroxo}) provides useful mechanistic insights into ferritin mineralization and demonstrates a flexible ferroxidase site.

The function of ferritin is a unique example of biomineralization. The protein alone can effect the reversible phase transition of iron ions in solution to the mineral core. It serves to concentrate and oxidize the cytotoxic Fe^{2+} ions and store the oxidized Fe in an inner cavity as a ferric oxy−hydroxide mineral core (*1*−*3*). It is ubiquitous and can be found in practically all known organisms including animals, plants, and microorganisms. Except for the 12-subunit form found in the bacterium *Listeria innocua* (*4*, *5*), ferritins are 24-mers forming a hollow sphere with an outer and inner diameter of ∼120 and ∼80 Å, respectively. Ferritin molecules from vertebrates are heteropolymers composed of two types of subunits, H and L, which differ slightly in their amino acid sequences but exhibit distinct rates of Fe uptake; in the presence of O_2, the H subunit oxidizes Fe at a rate that is more than 1000-fold faster than that of the L subunit (*6*−*8*). In amphibian and swine, a second H-type subunit, termed M or H′, has been found (*2*, *9*). Ferritins from invertebrates, plants, and bacteria have sequences more similar to H than to L. A fourth type of ferritin found in bacteria, called bacterioferritin, contains heme groups that bridge pairs of subunits in the 24-mer molecule (*10*). Regardless of the subunit type and composition, all ferritin molecules have similar molecular structures with the subunits folded into structurally homologous four α helix bundles (*11*−*14*).

The ability of H subunits to promote rapid oxidation of Fe^{2+} is known as the ferroxidase activity. Measurements of the reaction stoichiometry performed at low Fe loadings (<24 Fe^{2+}/24-mer) using mass spectrometry, pH stat, and electrode oxymetry yielded an Fe^{2+}:O_2 ratio of 2:1 and an Fe^{2+}:H^+ ratio of 1:2, suggesting a two-electron reduction of O_2 to hydrogen peroxide for the ferritin ferroxidase reaction (*6*, *8*, *15*−*18*). Production of H_2O_2 was confirmed by the observation that addition of catalase increases the Fe^{2+}:O_2 stoichiometry from 2:1 to 4:1 (*6*, *15*). X-ray crystallographic

† This work was supported by NIH Grants GM 58778 (to B.H.H.) and DK 20251 (to E.C.T.).

* To whom correspondence should be addressed. B.H.H.: phone, 404-727-4295; fax, 404-727-0873; e-mail, vhuynh@emory.edu. E.C.T.: phone, 510-450-7670; fax, 510-597-7131; e-mail, etheil@chori.org.

‡ Emory University.

§ Children's Hospital Oakland Research Institute.

|| Current address: Department of Biochemistry and Molecular Biology, The Pennsylvania State University, University Park, PA 16802.

⊥ Current address: Departmento de Quimíca, Faculdade de Ciências e Tecnologia, Universidade Nova de Lisboa, 2825 Monte de Caparica, Portugal.

10.1021/bi026478s CCC: $22.00
Published on Web 10/12/2002

measurements of recombinant H-type ferritins (*10*, *13*, *14*) and kinetic investigations of site-specific variants (*8*, *19*−*21*) have identified the ferritin ferroxidase site as a binuclear Fe-binding site with a structure similar to those observed in O_2-activating non-heme diiron enzymes (*22*−*24*). In accordance with a binuclear ferroxidase site, Mössbauer investigations of Fe deposition in H-type ferritins at low Fe loadings showed formation of μ-oxo/μ-hydroxo diferric species as the ferroxidase products (*7*, *25*−*29*). Further insight into the ferritin ferroxidase mechanism was achieved by studying Fe protein interactions in recombinant frog M ferritin using stopped-flow absorption (*30*) and rapid freeze−quench Mössbauer spectroscopy (*31*), which showed the rapid formation (within 25 ms) of a blue transient diferric−peroxo intermediate (F_{peroxo}),[1] displaying an absorption maximum at 650 nm and characteristic Mössbauer parameters. Characterizations by resonance Raman (*32*) and EXAFS (*33*) of F_{peroxo} revealed a μ-1,2 binding mode for the bridging peroxide and an unusually short Fe−Fe distance of 2.53 Å. This unusual structure was postulated to strengthen the peroxide O−O bond and thus to promote the release of H_2O_2 during decay of F_{peroxo} (*33*). Similar intermediates absorbing in the 650 nm region have also been observed for other H-type ferritins (*20*, *34*). Very recently, a rapidly forming transient diferric−peroxo species that displayed Mössbauer and kinetic properties similar to those of F_{peroxo} in M ferritin was found during Fe oxidation catalyzed by recombinant human H ferritin (*35*). Taken together, the above observations suggest that these H-type ferritins share a common ferroxidase mechanism.

Recently, the production of H_2O_2 at the ferroxidase site was questioned by Lindsay et al. (*36*), who failed to detect H_2O_2 production during Fe deposition in horse spleen ferritin at low Fe loadings. Three different analytical methods, including a sensitive fluorometric method, were used in their study. More recently, however, Zhao et al. (*37*) have provided explanations for the failure of Lindsay et al. (*36*) to detect H_2O_2 in their measurements. One explanation was the use of horse spleen ferritin, which has a low H subunit content (2−4 H subunits/24-mer), resulting in low H_2O_2 production. Another involved the ability of H_2O_2 to react with components present in the ferritin reaction solution, and thus the order that Fe and the assay reagents are added was shown to be important. In Lindsay's experiments, the reagents were added at least 10 s (mostly minutes) after Fe was added. It was suggested that, by that time, the small amount of H_2O_2 produced would have been consumed by its reaction with components in the ferritin solution. By introducing the fluorescence reagents prior to the addition of Fe, Zhao et al. (*37*) were able to detect the H_2O_2 produced by horse spleen ferritin, as well as by recombinant human H ferritin. However, only about one-third of the predicted H_2O_2 produced was detected.

In our continuing effort to elucidate the molecular mechanism of ferritin ferroxidase reaction, establishing the reaction stoichiometry is essential, and thus quantitative determination of the H_2O_2 produced is required. To this end, we have employed a horseradish peroxidase-catalyzed spectrophotometric assay to quantify the amount of H_2O_2 produced during the ferroxidase reaction of frog M ferritin at low Fe loadings, and we have used rapid freeze−quench Mössbauer spectroscopy to monitor the accumulation and decay of F_{peroxo}. For the quantification of H_2O_2, the rapid mixing technique used in the rapid freeze−quench method was used to ensure the experimental conditions were identical to those of the Mössbauer measurements; thus the results can be correlated directly. A linear correlation between the H_2O_2 produced and the F_{peroxo} accumulated was found with a F_{peroxo}:H_2O_2 ratio of approximately 1.0. This result establishes unambiguously that H_2O_2 is indeed produced at the binuclear ferroxidase site via the decay of F_{peroxo}. The data also show that the decay of F_{peroxo} is accompanied by the parallel formation of multiple μ-oxo/μ-hydroxo diferric complexes, similar to those observed for other H-type ferritins, and small polynuclear clusters. Implications of these observations to the ferroxidase mechanism are discussed.

MATERIALS AND METHODS

Protein Purification. Recombinant apo M ferritin from frog was cloned and expressed in *Escherichia coli* and purified as previously described (*6*, *31*). The purified protein contains less than five endogenous Fe atoms per 24-mer, and thus removal of endogenous Fe by potentially interfering reductants (*20*) is not required, making the frog M ferritin particularly favorable for kinetic studies involving the ferroxidase site (*30*, *31*). Protein concentration was determined with the Bio-Rad assay using BSA (bovine serum albumin; Sigma-Aldrich) as standard. Protein preparations were used within 2 weeks of preparation.

Hydrogen Peroxide Assay. The H_2O_2 concentration was determined by a horseradish peroxidase-catalyzed spectrophotometric assay modified from the procedures described by Holt et al. (*38*). The assay solution contained 40 units/mL horseradish peroxidase, 5 mM 4-aminoantipyrine, and 10 mM vanillic acid in a buffer solution (0.2 M sodium chloride in 0.2 M MOPS buffer at pH 7.5) that was used for our ferritin Fe deposition experiments. During the assay, horseradish peroxidase uses H_2O_2 to oxidize 4-aminoantipyrene, the product of which condenses with vanillic acid to form a red quinone imine dye exhibiting a broad absorption band at 490 nm (Figure 1, inset) that can be easily followed with optical spectroscopy. The molar absorptivity of the quinone imine dye at 490 nm under these experimental conditions was determined as follows. A standard H_2O_2 solution of known concentration (3.8%; Molecular Probes) and the buffer solution were used to prepare solutions of H_2O_2 of variable concentrations that cover the range (0−2 mM) expected for the H_2O_2 generated in the ferritin Fe deposition experiments. Aliquots of the prepared H_2O_2 solutions (100 μL each) were then mixed with 700 μL of the assay solution in an optical cuvette, and the absorbance at 490 nm was measured. A linear dependence of the absorbance with the H_2O_2 concentration was found (Figure 1). The slope of this linear dependence yields the molar absorptivity, which was determined to be 6990 M^{-1} cm^{-1}. To investigate the rate that H_2O_2 was converted to the quinone imine dye, we performed stopped-flow absorption measurements (Kinetic Instruments, Ann Arbor, MI) where known concentrations of H_2O_2 (40−100 μM) were mixed rapidly with the assay solution. The results indicated that

[1] Abbreviations: F_{peroxo}, diferric μ-1,2 peroxo reaction intermediate; EXAFS, extended X-ray absorption fine structure; MOPS, 3-morpholinopropanesulfonic acid; T, tesla.

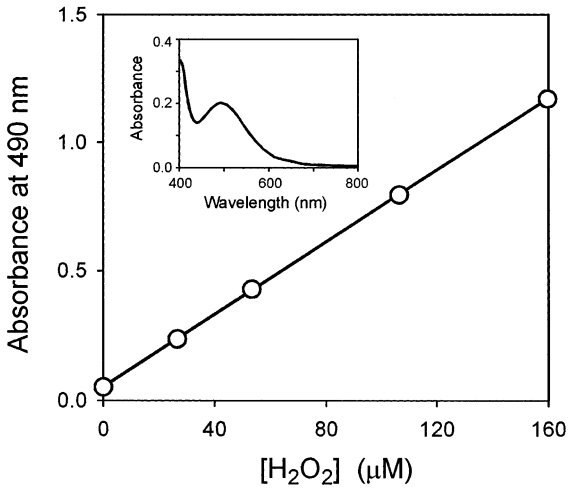

FIGURE 1: Linear H_2O_2 concentration dependence of the absorbance at 490 nm of the quinone imine dye, generated by the horseradish peroxidase-catalyzed spectrophotometric assay (see text). The inset shows an optical spectrum of the red quinone imine dye.

H_2O_2 was completely converted to the quinone imine dye in less than 500 ms under the current assay conditions.

Quantification of H_2O_2 Produced by the M Ferritin Ferroxidase Reaction. For the quantification of H_2O_2 generated during the ferroxidase reaction, an Update Instruments freeze−quench apparatus, which has been described elsewhere (*29*, *31*, *39*), was used to rapidly mix a solution of apoferritin (with varying concentration ranging from 34.6 to 86.7 μM in 0.2 M NaCl and 0.2 M MOPS buffer, pH 7.5) with an equal volume of $FeSO_4$ solution [in approximately 3.6 mM H_2SO_4 and 0.2 M NaCl; concentration of Fe determined by the ferrozine assay (*39*)] at 25 °C in a mixing chamber. Both solutions were oxygenated to saturation (∼1.2 mM in O_2) under 1 atm of O_2 prior to mixing. The reaction was allowed to proceed for 70 ms in an aging hose before 105 μL of the reaction mixture was sprayed into an optical cuvette containing 700 μL of the assay solution described above. Optical spectra of the solution in the cuvette were taken immediately in a Shimadzu UV 1601 spectrophotometer.

Determination of F_{peroxo} Accumulated. For the determination of the amount of F_{peroxo} accumulated during the ferroxidase reaction, the same apoferritin and iron solutions used for the H_2O_2 quantification measurements described above were used. Equal volumes of the two reactant solutions were mixed rapidly and efficiently by using the freeze−quench apparatus and were allowed to react for 35 ms, when the mixture would contain Fe only in the form of Fe(II) and F_{peroxo}. (Earlier studies have shown that a maximum amount of F_{peroxo} accumulates at a reaction time between 25 and 70 ms.) The reaction was then rapidly quenched by spraying the reaction mixture into cold isopentane (−140 °C), and the frozen samples of the reaction mixture were packed into Mössbauer cells for analysis as previously described (*29*, *31*, *39*). Mössbauer spectra of the samples were recorded at 4.2 K in a magnetic field of 50 mT applied parallel to the γ beam. Under these experimental conditions, F_{peroxo} exhibits a quadrupole doublet with characteristic parameters (see Results). The amount of F_{peroxo} accumulated in the reaction can then be determined from the relative absorption area of this doublet together with the total amount of Fe^{2+} added in the reaction.

Preparation of Freeze−Quench Mössbauer Samples for the Investigation of the Ferritin Ferroxidase Reaction. The rapid freeze−quench apparatus was also used to prepare Mössbauer samples for the study of the first second of the ferroxidase reaction. Again, an O_2-saturated solution of apo M ferritin (99 μM in 0.2 M NaCl and 0.2 M MOPS buffer, pH 7.5) was rapidly mixed with an equal volume of O_2-saturated Fe^{2+} solution (in 0.2 M NaCl and approximately 3.6 mM H_2SO_4). The Fe-to-protein ratio was fixed at 36 Fe: ferritin 24-mer. The reactants were allowed to react for a fixed period of time (0.035, 0.060, 0.125, 0.220, or 1 s) before being sprayed into cold isopetane at −140 °C. The frozen samples were then packed into Mössbauer cells for analysis.

Mössbauer Spectroscopy. Both the weak-field and strong-field Mössbauer spectrometers have been described elsewhere (*39*). Analysis of the spectra was conducted by using the WMOSS program (WEB Research Co., Edina, MN) based on a spin Hamiltonian formalism.

RESULTS

Reaction of H_2O_2 with Components Present in the Ferritin Reaction Mixture. For the quantification of H_2O_2 produced during the M ferritin ferroxidase reaction, we employed the rapid freeze−quench apparatus for rapid mixing of the reactants (see Materials and Methods). Our reasons for doing so were twofold: (1) to control accurately the time of reaction between apoferritin and Fe^{2+} and (2) to ensure the mixing conditions for the H_2O_2 determination were identical to those of the freeze−quench Mössbauer measurements, so that the results of both measurements can be correlated directly. As it turned out, rapid and efficient mixing using the freeze−quench apparatus was absolutely essential for the quantitative analysis of the H_2O_2 generated during the ferroxidase reaction. To determine the optimal time for apoferritin to react with Fe^{2+} before assay addition, we varied the reaction time from 70 ms (where the accumulation of F_{peroxo} is near or at its maximum) to 30 s (where the decay of F_{peroxo} is complete) and determined the amount of H_2O_2 in the reaction mixture as a function of the reaction time. The results are presented in Figure 2. In this experiment, the Fe-to-protein ratio was kept in the low Fe loading region and fixed at 11 Fe^{2+}/ferritin 24-mer. This was to ensure that most of the Fe^{2+} added would be oxidized via the binuclear ferroxidase center. (In principle, each ferritin molecule can bind up to 48 ferrous atoms in its 24 binuclear ferroxidase sites.) In Figure 2, the amount of H_2O_2 detected in the reaction mixture is normalized by the total amount of Fe added. A $[H_2O_2]$:[Fe] value of 0.5 represents stoichiometric production of H_2O_2 (i.e., one H_2O_2 produced by two Fe atoms). It can be seen that within a reaction time of 100 ms this value is approached. [In practice, the theoretical value of 0.5 is unattainable because not all the added Fe^{2+} will form F_{peroxo}, the presumed precursor of H_2O_2 (vide infra and ref *31*)]. When the Fe^{2+} and apoferritin are allowed to react for 1 s before the addition of the assay solution, the amount of H_2O_2 detected decreases by approximately 30%, and by a 10 s reaction time, less than 20% of the H_2O_2 generated remains in solution. This observation indicates that, in the presence of apoferritin, Fe^{2+}, and O_2, the H_2O_2 generated during the ferroxidase reaction is unstable and may react with either one or several of the components in the reaction

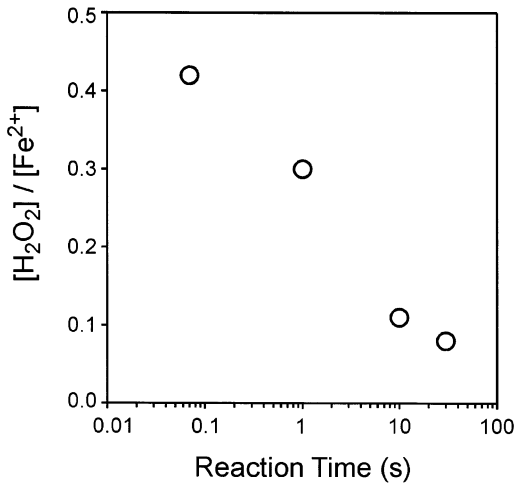

FIGURE 2: Amount of H_2O_2 detected in the reaction mixture as a function of the reaction time. The concentration of H_2O_2 is normalized with respect to the concentration of the total Fe^{2+} added to the solution. The decrease in the detectable H_2O_2 concentration with time suggests that H_2O_2 is consumed by reacting with components present in the mixture.

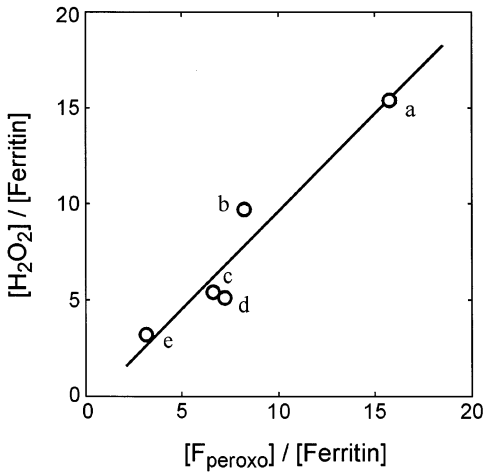

FIGURE 3: Linear correlation between the production of H_2O_2 and the accumulation of F_{peroxo} during the M ferritin ferroxidase reaction. The letters label the data points listed in Table 1. Linear regression of the data yields the solid line with a slope of 1.01 ± 0.17, an ordinate intercept of -0.54 ± 1.5, and a correlation coefficient $r = 0.96$.

Table 1: Key Experimental Values for the Data Presented in Figure 3

data point	ferritin 24-mer concn (μm)	added Fe^{2+}/ferritin	F_{peroxo} Mössbauer absorption (%)	$[F_{peroxo}]$/[ferritin]	$[H_2O_2]$/[ferritin]
a	87	35	90	15.8	15.4
b	67	30	55	8.2	9.7
c	41	30	44	6.6	5.4
d	35	36	40	7.2	5.1
e	67	11	60	3.2	3.2

mixture. Reaction of H_2O_2 with components present in the reaction mixture containing other ferritins, such as horse spleen ferritin and recombinant human ferritin, has also been observed (*37*). Therefore, for an accurate quantification of the H_2O_2 produced during the decay of F_{peroxo}, it is important to introduce the assay solution at or immediately after the accumulation of F_{peroxo} reaches its maximum and when the production of H_2O_2 begins. On the basis of the above observation, a reaction time of 70 ms was used for all of the H_2O_2 quantification measurements reported in this study. Consequently, rapid mixing using the rapid freeze−quench apparatus is required in order to control the reaction time down to the millisecond time scale.

Linear Correlation between the Production of H_2O_2 and the Amount of F_{peroxo} Accumulated during M Ferritin Ferroxidation. Rapid freeze−quench Mössbauer measurements (*31*) have shown that reaction of recombinant frog M apoferritin with Fe^{2+} in the presence of O_2 generates, within the millisecond time scale (25−70 ms), a diferric μ-1,2 peroxo intermediate, F_{peroxo}, the decay of which has been postulated to produce H_2O_2 and oxy−ferric dimers (mineral precursors) (*31*, *33*). To demonstrate that H_2O_2 is indeed a decay product of F_{peroxo}, we quantified the amount of H_2O_2 produced during the ferroxidase reaction and correlated the results with the amount of F_{peroxo} accumulated under the same reaction conditions. The production of H_2O_2 was quantified by a horseradish peroxidase-catalyzed spectrophotometric assay, and the accumulation of the diferric−peroxo intermediate, F_{peroxo}, was determined by rapid freeze−quench Mössbauer spectroscopy (see Materials and Methods). Three different preparations of apo M ferritin were used in these measurements, with varying Fe-to-protein ratios, resulting in five data points presented in Figure 3. Table 1 lists the values of the key experimental variables and Mössbauer results that lead to these five data points. Both the measured H_2O_2 and F_{peroxo} concentrations were normalized with their respective ferritin concentrations. A linear correlation between the concentrations of H_2O_2 and F_{peroxo} is observed. A least-squares fit of the data, assuming linear dependence, yields a slope of 1.01 ± 0.17 $[H_2O_2]/[F_{peroxo}]$ (solid line in Figure 3). Thus, the data indicate clearly that one H_2O_2 molecule is generated per decay of each F_{peoxo} complex, confirming our previous postulation.

Production of μ-Oxo/μ-Hydroxo Ferric Dimers and Small Polynuclear Clusters Resulting from Decay of F_{peroxo}. An advantage of using Mössbauer spectroscopy to study the ferritin ferroxidase reaction is the ability to probe all forms of iron complexes present in the reaction mixture. Although the spectra can be complex, there is the possibility to follow the transformation of one form of iron species into the other as the reaction advances and thus obtain useful mechanistic insights. A previous rapid freeze−quench Mössbauer investigation on the ferroxidase reaction of M ferritin has revealed the biphasic oxidation of Fe^{2+} and the accumulation of a rapidly forming transient reaction intermediate, F_{peroxo} (*31*). A major aim of the present study was to ascertain the initial product(s) formed following the decay of F_{peroxo}. To this end, 99 μM apoferritin was reacted with the equilvalent of 36 Fe/ferritin 24-mer under O_2-saturated conditions, and the reaction was quenched at 0.035, 0.060, 0.125, 0.220, or 1 s for Mössbauer investigations. Figure 4 shows the Mössbauer spectrum (hatched marks) of the 35 ms sample recorded at 4.2 K in a field of 50 mT applied parallel to the γ beam. Two quadrupole doublets, one major and one minor, are observed. The major doublet (solid line in Figure 4) accounting for 85% of the total Fe absorption arises from F_{peroxo}, and the minor doublet (indicated by a bracket) accounting for 15% of the total Fe absorption represents the slowly reacting Fe^{2+}. Consistent with our previous investigation (*31*), this observation indicates that within 35 ms a

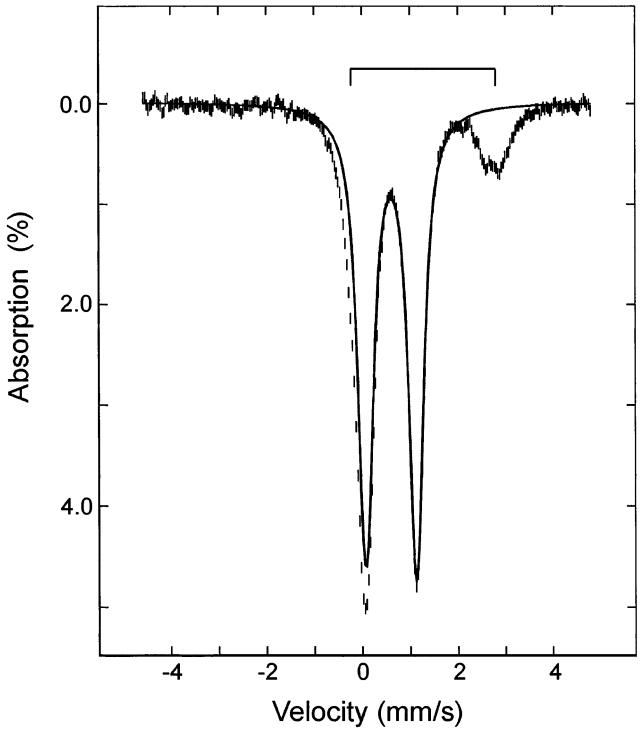

FIGURE 4: Mössbauer spectrum of a rapid freeze−quenched sample from the reaction of recombinant frog M ferritin with Fe^{2+} (36 Fe/ferritin 24-mer) and O_2. The reaction was quenched at 35 ms. The spectrum (hatched marks) was recorded at 4.2 K in a magnetic field of 50 mT applied parallel to the γ beam. The solid line is a theoretical simulation of the spectrum of F_{peroxo} using the parameters listed in Table 2 and scaled to 85% of the total Fe absorption. The bracket indicates the positions of the quadrupole doublet arising from the slowly reacting Fe^{2+}, accounting for the other 15% of the absorption.

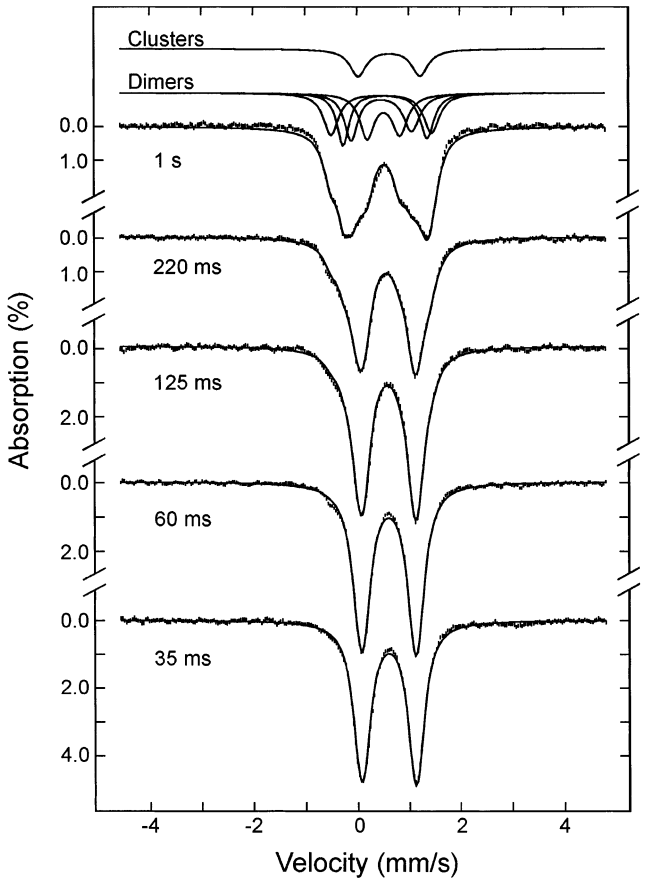

FIGURE 5: Time-dependent Mössbauer spectra from the reaction of recombinant frog M ferritin with Fe^{2+} (36 Fe/ferritin 24-mer) and O_2. The samples were prepared by the rapid freeze−quench method, and the reaction was quenched at the times indicated in the figure. The spectra (hatched marks) were recorded at 4.2 K in a parallel magnetic field of 50 mT. For clarity, contributions from the slowly reacting Fe^{2+} have been removed from these spectra. The solid lines overlaid with the experimental spectra are theoretical simulations using the parameters and absorption percentages listed in Table 2. The individual theoretical spectra of the μ-oxo/μ-hydroxo ferric dimers and small polynuclear clusters for the 1 s sample are shown on top of the spectrum.

majority (85%) of the Fe^{2+} is rapidly converted into F_{peroxo}. To examine the transformation of F_{peroxo} into its decay products, spectra of samples quenched at longer reaction times were recorded at 4.2 K in a parallel field of 50 mT and are displayed in Figure 5 (hatched marks). For clarity, the contributions from the slowly reacting Fe^{2+} component were removed from these spectra. As expected, at 35 and 60 ms reaction times, the spectra consist of mainly the quadrupole doublet arising from F_{peroxo} (compare with Figure 4), but by 125 ms significant broadening of the spectrum is observed and shoulders start to develop on the outer edges of the spectral envelope while the doublet associated with F_{peroxo} decreases in intensity. By 1 s the spectrum can be clearly seen as the sum of several overlapping quadrupole doublets arising from the decay products of F_{peroxo}. To further characterize these decay products, Mössbauer spectra of these samples were also recorded in a strong parallel field of 8 T at 4.2 K and are shown in Figure 6 (hatched marks). These strong-field spectra indicate that a majority of the decay products are diamagnetic, exhibiting absorption in the region between −2 and +2.5 mm/s, while a minor portion of the decay products are paramagnetic, exhibiting broad absorptions extending from −8 to +9 mm/s. These broad absorptions associated with the paramagnetic decay products are most clearly observed in the spectrum of the 1 s sample (Figure 6). However, it is noted that the presence of the paramagnetic products, although small in quantity, is already detectable in the 125 ms sample (Figure 6).

To obtain a quantitative measure for the conversion of F_{peroxo} to its decay products, we performed a global, iterative analysis (described in refs *29* and *31*) of both the weak-field and strong-field spectra. The results are presented in Table 2 and Figure 7. Theoretical spectra simulated with the parameters listed in Table 2 are plotted as solid lines in Figures 5 and 6. During the analysis, it was found that, at a minimum, four quadrupole doublets with comparable intensities are required to properly simulate the spectra of the diamagnetic products. To reduce the number of variable parameters, the intensities of these four quadrupole doublets are assumed to be equal. The Mössbauer parameters (ΔE_Q and δ) thus obtained indicate high-spin ferric ions, and the observed diamagnetism suggests that these ferric ions are antiferromagnetically coupled to form diferric complexes. The presence of multiple quadrupole doublets indicates a distribution in the ligand environment of these binuclear Fe products. On the basis of protein and model compound studies (*40*), μ-oxo diferric complexes generally yield larger ΔE_Q values (1.4−2.4 mm/s) than those (0.6−1.0 mm/s) of μ-hydroxo diferric complexes. The range of ΔE_Q observed for the diamagnetic decay products (0.67−1.67 mm/s)

Table 2: Mössbauer Parameters for the Fe Species Generated during the M Ferritin Ferroxidase Reaction and Their Percent Mössbauer Absorptions at Various Reaction Times

species	ΔE_Q (mm/s)	δ (mm/s)	η	% absorption[a] 0.035 s	0.060 s	0.125 s	0.220 s	1.0 s
F_{peroxo}[b]	−1.05	0.65	0.7	85	82	67	44	∼0
	−1.06	0.55	0.7					
dimers	−1.95	0.48	0.5	0	4	15	33	63
(μ-oxo/μ-hydroxo	−1.63	0.55	0.2					
diferric complexes)	−1.17	0.48	0.0					
	0.63	0.52	0.9					
small clusters	∼1.20	∼0.63		0	2	9	16	32

[a] Percent absorptions estimated for the slowly reacting Fe^{2+} are 15, 12, 9, 7, and 5, respectively, at reaction times 0.035, 0.060, 0.125, 0.220, and 1 s. [b] To better simulate the shape of the spectrum of F_{peroxo}, two overlapping quadrupole doublets were used.

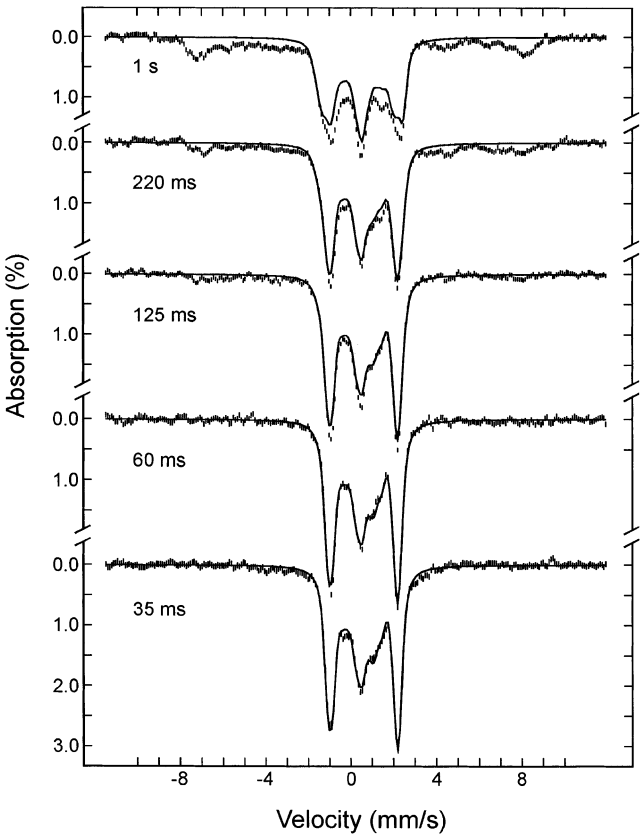

FIGURE 6: Strong-field Mössbauer spectra of rapid freeze−quenched samples from the reaction of recombinant frog M ferritin with Fe^{2+} and O_2. The samples are the same as those of Figure 5 with quenching times indicated in the figure. The spectra (hatched marks) were recorded at 4.2 K with a parallel applied field of 8 T. Contributions from the slowly reacting Fe^{2+} have been removed from these spectra. The solid lines overlaid with the experimental spectra are superpositions of the theoretical spectra of F_{peroxo} and the ferric dimers simulated with parameters and percent absorptions listed in Table 2.

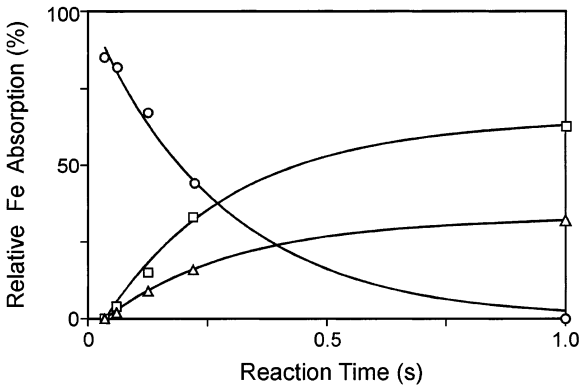

FIGURE 7: Time dependence of the Fe species observed during the M ferritin ferroxidase reaction (36 Fe/ferritin 24-mer) monitored by Mössbauer spectroscopy. The data show that the decay of F_{peroxo} (circles) is accompanied by the formation of ferric dimers (squares) and small clusters (triangles). The solid lines are kinetic traces using the parameters obtained from Figure 8.

suggests that both oxo- and hydroxo-bridged dimers are produced during the decay of F_{peroxo}. For the paramagnetic products, the 8 T spectra of the 220 ms and 1 s samples (Figure 6) show a distribution of internal field in the range of 45−50 T. In a weak applied field (e.g., 50 mT), the spectrum of the paramagnetic products partially collapses into a quadrupole doublet, of which the parameters were estimated from the weak-field spectra of the 220 ms and 1 s samples, and are listed in Table 2. The observed distribution in internal field and collapse of the paramagnetic spectrum observed at strong field into a quadrupole doublet at weak field are consistent with the paramagnetic products being small polynuclear clusters. (On the basis of the Fe absorption, a nuclearity of 8−12 was estimated for these clusters.) In the study of the frog H-L134P variant, a trinuclear Fe cluster exhibiting paramagnetic spectra at strong field (>4 T) was found among the initial ferroxidase products (*29*). We have therefore investigated the possibility that the paramagnetic component observed here for the M ferritin may also be a trimer. Analysis of spectra recorded at various applied fields (4−8 T) shows that the paramagnetic component of M ferritin exhibits field dependence inconsistent with that of the trimer mentioned above (*29*).

The time dependence of the relative proportions of the different Fe species described above is illustrated in Figure 7 where percent absorptions of the various species (F_{peroxo}, dimers, and small polynuclear clusters) are plotted as a function of reaction time. The transient nature of F_{peroxo} is clearly seen. As previously reported (*31*), it forms rapidly, reaching its maximum accumulation at 25−70 ms, and decays gradually to zero within 1 s. The decay of F_{peroxo} is accompanied by the formation of the dimers and small polynuclear Fe clusters. Analysis of the data indicates that the decay of F_{peroxo} is first order. A plot of the natural log of the percent absorption of F_{peroxo} as a function of the reaction time (Figure 8A) shows a linear dependence. Linear regression yields a slope of $-(3.62 \pm 0.36)$ s^{-1} for the decay rate of F_{peroxo}. To show that the formation of the dimers and the polynuclear clusters is parallel to the decay of F_{peroxo}, we plot in Figure 8B $\log(A_{final} - A)$ of both species versus

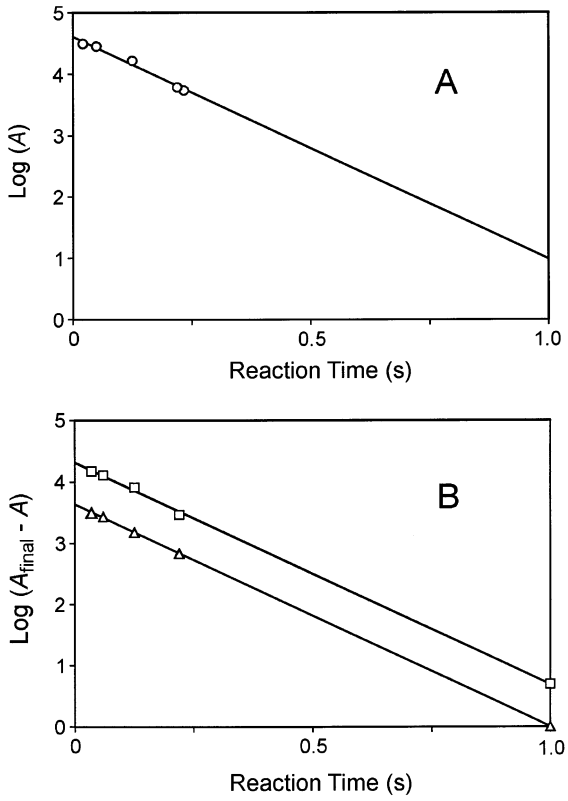

FIGURE 8: First-order dependence of the decay of F_{peroxo} (A) and the formation of dimers and small polynuclear clusters (B) during the M ferritin ferroxidase reaction (36 Fe/ferritin 24-mer). Panel A: Plot of natural log of percent absorption, *A*, of F_{peroxo} as a function of reaction time. Linear regression analysis yields the solid line shown, which has a slope of -3.62 ± 0.36, an ordinate intercept of 4.61 ± 0.05, and a correlation coefficient $r = 0.99$. Panel B: Plots of log of ($A_{final} - A$) for the dimers (squares) and small clusters (triangles), where *A* represents the percent absorption of each species and A_{final} is a fitting parameter. Linear regression yields the two solid lines shown with slope $= -3.63 \pm 0.06$, intercept $= 4.32 \pm 0.03$, $r = 1.0$, and $A_{final} = 65\%$ for the dimers and with slope $= -3.64 \pm 0.02$, intercept $= 3.64 \pm 0.01$, $r = 1.0$, and $A_{final} = 33\%$ for the small clusters.

reaction time, where *A* represents the percent absorption of either species. Again, a linear time dependence is observed for both products, indicating a first-order formation rate. Least-squares fits to the data yield rate constants of (3.63 ± 0.06) s^{-1} and (3.64 ± 0.02) s^{-1} for the dimers and clusters, respectively. Thus, the data indicate unambiguously that the decay of F_{peroxo} generates both the diferric oxo/hydroxo dimers and the small polynuclear clusters, *with the same rate*. In Figure 7, the solid lines overlaid with the experimental data are theoretical simulations using the parameters obtained from this analysis.

DISCUSSION

Product identification and reaction stoichiometries are among the most important information required for the understanding of reaction mechanisms. Using mass spectrometry, electrode oxymetry (coupled with the effects of catalase) (*6*, *8*, *15*, *16*, *37*, *41*), and Mössbauer spectroscopy (*7*, *26*−*29*, *31*, *35*), previous investigators have identified H_2O_2 and multiple diferric oxo/hydroxo species as the first products of ferritin ferroxidase reaction (see the introduction). However, the relation between the product H_2O_2 to its precursor, F_{peroxo}, was not clear, and stoichiometric quantification of H_2O_2 produced during the reaction has proven to be difficult to achieve because H_2O_2 reacts with components in the reaction mixture (see Figure 2 and ref *37*). Indeed, Lindsay et al. were unsuccessful in their attempt to detect any H_2O_2 released by horse spleen ferritin and concluded that H_2O_2 was not a product of the reaction (*36*). The low H-subunit content of horse spleen ferritin (2−4 H subunits/24-mer) and losses of H_2O_2 due to its interaction with components in the mixture likely combined to decrease the amount of H_2O_2 below the limits of detection of the analysis. When H_2O_2 trapping reagents were introduced prior to the addition of iron, release of H_2O_2 by horse spleen ferritin was observed (*37*), although at 33% of the predicted value (one H_2O_2 molecule produced per two Fe atoms added). The reason for this partial detection of H_2O_2 is not known. One possible explanation could be that the assay reagents are competing with ferritin for the added Fe, and this affects the formation of F_{peroxo}, which is the precursor of H_2O_2. In the current study, we use an enzymatic assay that reacts immediately and specifically with H_2O_2 to produce a stable organic derivative that can be easily monitored by absorption spectroscopy. To prevent H_2O_2 from reacting with components of the reaction mixture and to avoid assay reagents interfering with the formation of F_{peroxo}, we employed the rapid freeze−quench apparatus to rapidly mix the reactants and introduce the assay 70 ms after mixing. At this time the accumulation of F_{peroxo} is complete, and therefore addition of the assay does not interfere with the formation of F_{peroxo}. Furthermore, it allows the H_2O_2 analysis to begin just as F_{peroxo} starts to decay and H_2O_2 is released. By doing so, we were able to quantitatively detect most, if not all, of the H_2O_2 produced and correlate the result with the amount of F_{peroxo} accumulated in the reaction (determined by Mössbauer spectroscopy). The production of H_2O_2 was found to be linearly related to the amount of F_{peroxo} accumulated with a stoichiometry of approximately 1 (see Figure 3). This result indicates not only that H_2O_2 is produced during the ferritin ferroxidase reaction but also that the $[H_2O_2]/[F_{peroxo}]$ stoichiometry further supports our proposal that H_2O_2 is a decay product of the reaction intermediate F_{peroxo} (*31*, *33*). Spectroscopic investigations (*31*−*33*) have established that F_{peroxo} is a diferric μ-1,2 peroxo complex with an unusually short Fe−Fe distance of 2.53 Å and a relatively sharp Fe−O−O angle of 107°. This unusual geometry of F_{peroxo} was hypothesized (*33*) to strengthen the O−O bond and thus favor protonation of the peroxo bridge, triggering release of H_2O_2 in contrast to the O−O bond cleavage observed in several O_2-activating diiron enzymes, which form high-valence diiron species for oxidation of organic substrates (*24*). The H_2O_2:F_{peroxo} stoichiometry of 1 found in this study is in support of such a mechanistic hypothesis. Furthermore, previous stoichiometric investigations into the ferroxidase reaction of H-type ferritins (*6*, *15*) have shown that the number of Fe oxidized per O_2 consumed increases from 2 to 4 in the presence of catalase, establishing that for each H_2O_2 produced two ferrous ions are oxidized. The H_2O_2:F_{peroxo} stoichiometry determined here is in perfect agreement with this previously determined stoichiometry, since F_{peroxo} is a diferric complex.

When the Fe products generated by the decay of F_{peroxo} were monitored by rapid freeze−quench Mössbauer spectroscopy, conversion of F_{peroxo} to multiple antiferromagneti-

cally coupled diferric complexes (dimers) and small ferric clusters was observed (Figures 7 and 8). On the basis of their Mössbauer parameters, the dimers are assigned to be oxo- and/or hydroxo-bridged diferric complexes. Diferric μ-oxo and μ-hydroxo complexes with Mössbauer parameters similar to those reported here were also observed as products of the ferroxidase reaction in other H-type ferritins, including human H ferritin, frog H ferritin (L134P variant), and *E. coli* non-heme bacterial ferritin (*20*, *26*−*29*, *31*, *42*). In agreement with results presented here and previously (*31*) for M ferritin, conversion of F_{peroxo} to these μ-oxo/μ-hydroxo dimers has also been observed very recently in the ferroxidase reaction catalyzed by recombinant human H ferritin (*35*). Formation of μ-oxo and/or μ-hydroxo dimers through the decay of F_{peroxo} by releasing H_2O_2 is a very probable process from a mechanistic point of view. On the basis of X-ray crystallographic data (*14*), water molecules are likely ligands for F_{peroxo}. Binding of H_2O to a cationic metal would reduce the pK_a of the water molecule, making it a potential proton donor to the bridging peroxide. Moreover, oxidation of Fe(II) to Fe(III) will further decrease the pK_a of the coordinated H_2O. The deprotonated water molecule could then occupy the bridge vacated by the release of the bridging peroxide (now protonated) and form the oxo or hydroxo bridge, depending on the degree of its deprotonation. In addition to the production of dimers, the data showed that the decay of F_{peroxo} also produces small polynuclear clusters. This observation is without precedent and rather difficult to envision mechanistically since the process would likely require coordinate release and complexation of binuclear precursors from multiple ferroxidase sites in different protein subunits.

The observation of multiple products generated by the decay of a single reaction intermediate, F_{peroxo}, establishes clearly that ferroxidation of H-type ferritin occurs at a specific binuclear site (the ferroxidase site), even though multiple decay products were detected. Possible explanations for the heterogeneity of the dimer products are many, including (1) a conformational distribution at the ferroxidase sites, (2) binding of the dimers to either one of the two Fe ligand sets (E, EXXH and E, QXXD) at the ferroxidase sites, and (3) binding of the dimers at the translocation sites. The fact that the formation rate of each product, rather than the sum of the formation rates of all products, is identical to the decay rate of F_{peroxo} suggests the likely existence of an intervening intermediate, which decays to the various products, and that the decay of F_{peroxo} to this intermediate is the rate-determining step. The observation of various products reflects the presence of multiple ferroxidase sites (a total of 24) within an H ferritin molecule and suggests different protein environments exist among these sites to allow for the different decay pathways. Previous rapid freeze−quench Mössbauer investigations into the ferroxidase reaction of the frog H-L134P variant (*29*) also showed parallel formation of multiple ferroxidase products, which was explained by the existence of flexible ferroxidase sites. However, this earlier investigation could not show that these multiple products were produced from a single precursor, because the precursor was not detected. The current study has thus provided the key information (multiple products from a single precursor) that demonstrates the structural plasticity of the ferroxidase site in H-type ferritin. Evidence supporting different protein environments at the multiple ferroxidase sites and flexibility of ferritin structures includes the observed biphasic rates of site restoration after oxidation of Fe (*6*, *20*), the asymmetric arrangement of subunits around the pores where Fe enters the protein (*11*, *14*, *43*), and changes in residue positions observed in protein crystals obtained under different crystallization conditions (*43*). The observed multiple decay pathways for F_{peroxo} (and its implication of different protein environments for the ferroxidase sites within a ferritin molecule) are in contrast to the highly specialized enzymatic reactions catalyzed by the O_2-activating non-heme diiron enzymes (*22*−*24*), which contain a diiron site similar to that of the ferroxidase site in H ferritins. In the diiron enzymes, which are designed to catalyze specific reactions, Fe is part of a cofactor, while in ferritin Fe is a substrate. The oxidized Fe in ferritin presumably vacates the ferroxidase sites (*6*, *20*) for translocation into the inner cavity. For such a function, a flexible Fe oxidizing site may be preferable. In this respect, it is important to note that all types of ferritins oxidize and concentrate Fe but employ different strategies. For example, bacteria have multiple ferritins with different Fe oxidation pathways that include the non-heme (mentioned above) and heme-containing ferritins (*44*). The heme-containing bacterioferritin in *E. coli* has a ferroxidase site with ligands (two EXXH sequences) homologous to those of the diiron enzymes (*45*) and uses O_2 to oxidize Fe to produce diferric μ-oxo/μ-hydroxo complexes at the ferroxidase site, but the oxidized Fe is retained at the ferroxidase site (*46*, *47*). Moreover, on the basis of electrode oxymetry/pH stat measurements the O_2 is reduced to water (*46*). Interestingly, a recent investigation (*48*) shows that the reduction of O_2 to water in *E. coli* bacterioferritin is achieved via two two-electron reduction steps with H_2O_2 being the intermediate product. The two pairwise reduction steps are suggested to take place in two separate diferrous-bound ferroxidase sites and thus avoid the formation of reactive odd-electron reduction products of O_2. The differences observed in the ferroxidase reaction pathways between bacterioferritin and vertebrate H-type ferritins are likely related to the differences in the ligand environments of their feroxidase sites. In bacterioferritin, each Fe is coordinated by a histidine and a glutamate residue and bridged by two carboxylate groups (E51 and E127) (*45*). In contrast, in H-type ferritins the metals are bridged by only one glutamate residue, and only one metal has histidine coordination, the other having a glutamate in place of the histidine (*13*, *14*). In addition, the ferroxidase site of H-type ferritins contains a conserved glutamine that is absent in bacterioferritin. Finally, a ferritin-like DNA binding protein found in *E. coli* uses H_2O_2 as a more efficient substrate to oxidize Fe^{2+} than O_2, suggesting a DNA protective function by using the ferroxidase reaction to eliminate the combined toxic effects of Fe^{2+} and H_2O_2 (*49*). Apparently, flexibility in protein structure, composition, and type is an inherent property of ferritin that allows it to adapt its function for specific cellular needs.

ACKNOWLEDGMENT

We thank one of the reviewers for suggesting a plausible mechanistic explanation for the parallel formation of the multiple decay products of F_{peroxo}.

REFERENCES

1. Theil, E. C. (2000) in *Handbook of Metalloproteins* (Messerschmidt, A., Huber, R., Poulos, T., and Wieghardt, K., Eds.) pp 771−781, John Wiley & Sons, Chichester, U.K.
2. Harrison, P. M., and Arosio, P. (1996) *Biochim. Biophys. Acta 1275*, 161−203.
3. Chasteen, N. D., and Harrison, P. M. (1999) *J. Struct. Biol. 126*, 182−194.
4. Stefanini, S., Cavallo, S., Montagnini, B., and Chiancone, E. (1999) *Biochem. J. 338*, 71−75.
5. Yang, X., Chiancone, E., Stefanini, S., Ilari, A., and Chasteen, N. D. (2000) *Biochem. J. 349*, 783−786.
6. Waldo, G. S., and Theil, E. C. (1993) *Biochemistry 32*, 13262−13269.
7. Bauminger, E. R., Harrison, P. M., Hechel, D., Nowik, I., and Treffry, A. (1991) *Biochim. Biophys. Acta 1118*, 48−58.
8. Sun, S., Arosio, P., Levi, S., and Chasteen, N. D. (1993) *Biochemistry 32*, 9362−9369.
9. Waldo, G. S., and Theil, E. C. (1996) in *Comprehensive Supramolecular Chemistry* (Suslick, K. S., Ed.) pp 65−89, Pergamon Press, Oxford, U.K.
10. Frolow, F., Kalb, A. J., and Yariv, J. (1994) *Nat. Struct. Biol. 1*, 453−460.
11. Lawson, D. M., Artymiuk, P. J., Yewdall, S. J., Smith, J. M. A., Livingstone, J. C., Treffry, A., Luzzago, A., Levi, S., Arosio, P., Cesareni, G., Thomas, C. D., Shaw, W. V., and Harrison, P. M. (1991) *Nature (London) 349*, 541−544.
12. Trikha, J., Waldo, G. S., Lewandowski, F. A., Ha, Y., Theil, E. C., Weber, P. C., and Allewell, N. M. (1994) *Proteins: Struct., Funct., Genet. 18*, 107−118.
13. Hempstead, P. D., Yewdall, S. J., Fernie, A. R., Lawson, D. M., Artymiuk, P. J., Rice, D. W., Ford, G. C., and Harrison, P. M. (1997) *J. Mol. Biol. 268*, 424−448.
14. Ha, Y., Shi, D., Small, G. W., Theil, E. C., and Allewell, N. M. (1999) *J. Biol. Inorg. Chem. 4*, 243−256.
15. Xu, B., and Chasteen, N. D. (1991) *J. Biol. Chem. 266*, 19965−19970.
16. Yang, X., Chen-Barrett, Y., Arosio, P., and Chasteen, N. D. (1998) *Biochemistry 37*, 9743−9750.
17. Treffry, A., Zhao, Z., Quail, M. A., Guest, J. R., and Harrison, P. M. (1998) *FEBS Lett. 432*, 213−218.
18. Yang, X., and Chasteen, N. D. (1999) *Biochem. J. 338*, 615−618.
19. Hempstead, P. D., Hudson, A. J., Artymiuk, P. J., Andrews, S. C., Banfield, M. J., Guest, J. R., and Harrison, P. M. (1994) *FEBS Lett. 350*, 258−262.
20. Treffry, A., Zhao, Z., Quail, M. A., Guest, J. R., and Harrison, P. M. (1995) *Biochemistry 34*, 15204−15213.
21. Treffry, A., Zhao, Z., Quail, M. A., Guest, J. R., and Harrison, P. M. (1997) *Biochemistry 36*, 432−441.
22. Wallar, B. J., and Lipscomb, J. D. (1996) *Chem. Rev. 96*, 2625−2657.
23. Feig, A. L., and Lippard, S. J. (1994) *Chem. Rev. 94*, 759−805.
24. Krebs, C., and Huynh, B. H. (1999) in *Iron Metabolism* (Ferreira, G. C., Moura, J. J. G., and Franco, R., Eds.) pp 253−273, Wiley-VCH, Weinheim.
25. Bauminger, E. R., Harrison, P. M., Nowik, I., and Treffry, A. (1989) *Biochemistry 28*, 5486-5493.
26. Bauminger, E. R., Harrison, P. M., Hechel, D., Hodson, N. W., Nowik, I., Treffry, A., and Yewdall, S. J. (1993) *Biochem. J. 296*, 709−719.
27. Bauminger, E. R., Treffry, A., Quail, M. A., Zhao, Z., Nowik, I., and Harrison, P. M. (1999) *Biochemistry 38*, 7791−7802.
28. Bauminger, E. R., Treffry, A., Quail, M. A., Zhao, Z., Nowik, I., and Harrison, P. M. (2000) *Inorg. Chim. Acta 297*, 171−180.
29. Pereira, A. S., Tavares, P., Lloyd, S. G., Danger, D., Edmondson, D. E., Theil, E. C., and Huynh, B. H. (1997) *Biochemistry 36*, 7917−7927.
30. Fetter, J., Cohen, J., Danger, D., Sanders-Loehr, J., and Theil, E. C. (1997) *J. Biol. Inorg. Chem. 2*, 652−661.
31. Pereira, A. S., Small, W., Krebs, C., Tavares, P., Edmondson, D. E., Theil, E. C., and Huynh, B. H. (1998) *Biochemistry 37*, 9871−9876.
32. Moënne-Loccoz, P., Krebs, C., Herlihy, K., Edmondson, D. E., Theil, E. C., Huynh, B. H., and Loehr, T. M. (1999) *Biochemistry 38*, 5290−5295.
33. Hwang, J., Krebs, C., Huynh, B. H., Edmondson, D. E., Theil, E. C., and Penner-Hahn, J. E. (2000) *Science 287*, 122−125.
34. Zhao, Z., Treffry, A., Quail, M. A., Guest, J. R., and Harrison, P. M. (1997) *J. Chem. Soc., Dalton Trans.*, 3977−3978.
35. Bou-Abdallah, F., Papaefthymiou, G. C., Scheswohl, D. M., Stanga, S. D., Arosio, P., and Chasteen, N. D. (2002) *Biochem. J. 364*, 57−63.
36. Lindsay, S., Brosnahan, D., and Watt, G. D. (2001) *Biochemistry 40*, 3340−3347.
37. Zhao, G., Bou-Abdallah, F., Yang, X., Arosio, P., and Chasteen, N. D. (2001) *Biochemistry 40*, 10832−10838.
38. Holt, A., Sharman, D. F., Baker, G. B., and Palcic, M. M. (1997) *Anal. Biochem. 244*, 384−392.
39. Ravi, N., Bollinger, J. M., Jr., Huynh, B. H., Stubbe, J., and Edmondson, D. E. (1994) *J. Am. Chem. Soc. 116*, 8007−8014.
40. Kurtz, D. M., Jr. (1990) *Chem. Rev. 90*, 585−606.
41. Sun, S., and Chasteen, N. D. (1992) *J. Biol. Chem. 267*, 25160−25166.
42. Treffry, A., Bauminger, E. R., Hechel, D., Hodson, N. W., Nowik, I., Yewdall, S. J., and Harrison, P. M. (1993) *Biochem. J. 296*, 721−728.
43. Trikha, J., Theil, E. C., and Allewell, N. M. (1995) *J. Mol. Biol. 248*, 949−967.
44. Hudson, A. J., Andrews, S. C., Hawkins, C., Williams, J. M., Izuhara, M., Meldrum, F. C., Mann, S., Harrison, P. M., and Guest, J. R. (1993) *Eur. J. Biochem. 218*, 985−995.
45. Frolow, F., Kalb, A. J., and Yariv, J. (1994) *Struct. Biol. 1*, 453−460.
46. Yang, X., Le Brun, N. E., Thomson, A. J., Moore, G. R., and Chasteen, N. D. (2000) *Biochemistry 39*, 4915−4923.
47. Le Brun, N. E., Wilson, M. T., Andrews, S. C., Guest, J. R., Harrison, P. M., Thomson, A. J., and Moore, G. R. (1993) *FEBS Lett. 333*, 197−202.
48. Bou-Abdallah, F., Lewin, A. C., LeBrun, N. E., Moore, G. R., and Chasteen, N. D. (2002) *J. Biol. Chem.* (in press).
49. Zhao, G., Ceci, P., Ilari, A., Giangiacomo, L., Laue, T. M., Chiancone, E., and Chasteen, N. D. (2002) *J. Biol. Chem.* (in press).

BI026478S